J. Membrane Biol. 136, 169–179 (1993)

The Journal of
Membrane
Biology

Cytoplasmic Acidosis Induces Multiple Conductance States in ATP-sensitive Potassium Channels of Cardiac Myocytes

Zheng Fan[1,2], Tetsushi Furukawa,[1] Tohru Sawanobori[1], Jonathan C. Makielski[2], Masayasu Hiraoka[1]

[1]Department of Cardiovascular Diseases, Medical Research Institute, Tokyo Medical and Dental University, 1-5-45 Yushima, Bunkyo-ku, Tokyo 113, Japan

[2]Cardiac Electrophysiology Laboratories, The University of Chicago, Chicago, Illinois 60637

Received: 11 March 1993/Revised: 22 June 1993

Abstract. We studied the effect of cytoplasmic acidosis on the ionic conducting states of ATP-sensitive potassium channels in heart ventricular cells of guinea pigs and rabbits by using a patch-clamp technique with inside-out patch configuration. Under normal conditions (pH 7.4), the channel alternated between a closed state and a main open state in the absence of nucleotides on the cytoplasmic side. As internal pH was reduced below 6.5, the single channel current manifested distinct subconductance levels. The probability of the appearance of these subconductance levels was pH dependent with a greater probability of subconductance states at lower pH. A variance-mean amplitude analysis technique revealed two subconductance levels approximately equally spaced between the main open level and the closed level (63 and 33%). A current-voltage plot of the two subconductance levels and the main level showed that they had similar reversal potentials and rectification properties. An intrinsic flickering gating property characteristic of these ATP-sensitive channels was found unchanged in the 63% subconductance state, suggesting that this subconductance state and the main conductance state share similar ion pore properties (including ion selection and block) and similar gating mechanisms. The appearance of the subconductance states decreased as ionic strength was increased, and the subconductance states were also slightly voltage dependent, suggesting an electrostatic interaction between the protons and the negative surface charge in the vicinity of the binding sites, which may be close to the inner entrance of the ion pore. Proteolytic modification of the channel on the cytoplasmic side with trypsin did not abolish the subconductance levels. External acidosis did not induce subconductance levels. These results suggest that protons bound to the negatively charged group at the inner entrance of the channel ion pore may induce conformational changes, leading to partially reduced conductance states.

Key words: ATP-sensitive K channel — Subconductance — Intracellular pH — Cardiac myocytes

Correspondence to: Z. Fan

Introduction

Intracellular acidification generally reduces the current passing through the ion pore in various kinds of K^+ channels (Cook, Ikeuchi & Fujimoto, 1984; Moody, 1984; Christensen & Zeuthen, 1987). A reduction of channel current can generally be attributed to either a decrease in the open probability of the channel, a decrease in unitary current amplitude, or both. The effect of cytoplasmic acidosis on I_{K1} provides an example (Ito, Vereecke & Carmeliet, 1992) where both mechanisms apply. For the ATP-sensitive K^+ channel ($I_{K,ATP}$) with ATP present in the cytoplasmic solution, low cytoplasmic pH antagonizes ATP inhibition of the channel, resulting in an increase of the channel activity (Davies, 1990; Standen et al., 1992; Fan & Makielski, 1993). However, for $I_{K,ATP}$ in the absence of ATP, low cytoplasmic pH causes a reduction in current similar to other K^+ currents. Low cytoplasmic pH reduced the open probability (unitary current amplitude not measured) of $I_{K,ATP}$ in pancreatic β-cells (Misler, Gillis & Tabcharani, 1989), decreased unitary cur-

Table. Composition of bathing and pipette solutions (in mM)

Solution[a]	K^+	Ca^{2+}	Mg^{2+}	Sucrose	Cl^-	Buffer[b]	EGTA
Bath (control)	144				144	5	2
Bath (low $[K^+]_i$)	10			300	10	5	2
Bath (high $[K^+]_i$)	300				300	5	2
Pipette	142	1.8	0.53		149	5	

[a] All solutions contained 5.5 mM glucose.
[b] HEPES for pH 7.4, PIPES for pH 6–7, MES for pH 5.2–6, acetic acid for 3.8–5. KOH and HCl were used for adjusting pH values, except for low $[K^+]_i$ solution in some experiments in which NaOH (≈5 mM) and HCl were used for adjusting pH values.

rent amplitude but without significant effect on open probability (up to pH 5.7) in $I_{K,ATP}$ of frog skeletal muscles (Davies, Standen & Stanfield, 1992), and reduced both open probability and unitary current amplitude in cardiac cells (Cuevas et al., 1991; Fan & Makielski, 1993). Here we report a novel mechanism for reduction of current by low cytoplasmic pH for $I_{K,ATP}$, namely, induction of subconductance states. This effect of cytoplasmic acidosis on $I_{K,ATP}$ channels has not been previously reported, and as far as we are aware, this is the first report that cytoplasmic protons induce multiple subconductance states in a K^+ channel.

Materials and Methods

Preparation

Single ventricular myocytes were isolated from guinea pig hearts by enzymatic dissociation (collagenase, type I, Sigma, St Louis, MO). The particular methods we used have previously been described in detail (Fan, Nakayama & Hiraoka, 1990a; El-Sherif, Fozzard & Hanck, 1992).

Solutions

The Table gives the composition of all bathing solutions (artificial intracellular medium), and the control pipette solutions (extracellular medium). We will refer to ion concentrations using brackets, and refer to the solution on the cytoplasmic side with a subscripted "*i*" and to the solution on the outside of the cell with a subscripted "*o*"; for example, $[K^+]_i$ denotes the intracellular or cytoplasmic potassium concentration. The pH of the solutions was adjusted to 7.4 with KOH (about 8 mM). The changes of pH in the solutions were performed by substitution of HEPES buffer with PIPES (pH 6–7), MES (pH 5.2–6), or acetic acid (pH 3.8–5), each at 5 mM. In some experiments, to exclude the possibility of additional effects of the buffers on the channels, the HEPES-buffered solution, for which pH changes were made by simply adding HCl, was used to confirm the results. No significant differences were found with HEPES buffer. Assuming that residual concentrations of Ca^{2+} and Mg^{2+} in the bathing solutions were nominally zero, free Ca^{2+} and Mg^{2+} were estimated to be less than 2×10^{-10} M and 5×10^{-6} M, respectively, as calculated from the apparent dissociation constants (Fabiato & Fabiato, 1979). All bathing solutions contained no ATP (ATP-free), except for those indicated otherwise. Under such conditions, the run-down of $I_{K,ATP}$ was relatively slow, and nearly stable channel activity could be maintained for over 10–20 min (Fan et al., 1990a). Solutions other than control solution were made fresh each experimental day. The bath solution could be replaced completely within 1 min. Experiments were carried out at a room temperature of 22–25°C.

Recording Methods

The patch-clamp technique was applied to record the current through single channels using a commercial patch-clamp amplifier (Axopatch-1D, Axon Instruments, Burlingame, CA). The current signals were amplified to 100–200 mV/pA and filtered through a built-in, 8-pole Bessel low-pass filter at a -3 dB frequency (f_c) and digitized at 5–30 kHz onto the disk of a computer (either Intel 80286 or 80486DX based) using a 12-bit analog-to-digital converter (AXON TL-1, Axon Instruments).

Since we used a Ag-AgCl-Cl^- electrode system with a liquid-solid surface, a change in $[Cl^-]$ of the solution would lead to a change in junction potential. To overcome this problem, the Ag-AgCl electrode for grounding was put into an agar-bridge of KCl (150 mM), which was immersed in bathing solution. At the start of each experiment, the junction potential of each electrode was nulled through adjustment of the compensation circuit.

Data Analysis

Only patches containing a single active channel were selected for analysis. This included some patches that showed multichannel activity early in the life of the patch, but only one functioning channel upon exposure to low intracellular pH (pH_i).

Single channel current data were analyzed and plotted using pCLAMP (Axon Instruments) and SigmaPlot (Jandel Scientific, San Rafael, CA) software. The unitary current amplitude was measured by two methods. A conventional amplitude histogram was constructed through all the points in a recorded file. Thereafter, the histogram was fitted to a sum of Gaussian distributions with individual means and variances. The difference between the means of two adjacent Gaussian peaks was taken as a measure of the difference in unitary current amplitude. Examination of amplitude histograms revealed that in many cases, especially when current fluctuated between subconductance levels, the

peaks were difficult to separate from each other. Therefore, a mean-variance analysis method (Patlak, 1988) was also used. The technique involved calculating a moving average current and variance in a window consisting of six data points with a sampling rate of 5 kHz. A running point by point mean and variance was calculated and a graph of this variance as a function of the mean current resulted in a family of parabolas between regions of low variance. These low-variance points typically indicated legitimate channel-current levels, while high-variance points represented either transitions between levels or very brief events. The criterion was set at the variance value of background noise at the closed level. Given such a variance level criterion, histograms could be constructed. In this study, a mean window current value with variance less than the variance of baseline (closed level) was selected as the criterion for a stable sojourn at a given level. The values at the peaks of each level in the histogram were taken as a measure of the current amplitude of the levels.

For detection of transition events, the detecting threshold was set at half the unitary or subconductance current level. Events were confirmed manually. Each distribution histogram of sojourn time was constructed from continuous recordings containing up to 3,000 events. A nonlinear optimal searching method using the least-squares principle was applied to fit the data with a probability density function having the form of an exponential distribution. The probability of a channel sojourn at a current level (P_j) was calculated by: t_j/T_d, where t_j is the time spent at that current level, and T_d is the duration of the recording being analyzed.

All data are presented as mean ± SEM. Paired t-test was used to test the significant difference at a P value less than 0.05.

Results

Cytoplasmic Acidosis Induced Subconductance of $I_{K,ATP}$

We have previously reported in freshly excised, inside-out patches at pH_i 7.4 that $I_{K,ATP}$ channels were opened nearly all of the time when ATP was absent from the internal solution. Also, the channel activity could be sustained over approximately 10 min in low $[Ca^{2+}]$ and $[Mg^{2+}]$ internal solution before it finally lost activity due to rundown (Fan et al., 1990*a*). When the internal pH was decreased to < 6.5, rundown was facilitated, but some $I_{K,ATP}$ remained active, although with a reduced unitary amplitude (Fig. 1). Figure 1 shows an example of channels active in low pH_i. The pH was measured to be pH 4.7 with HEPES buffer used in the internal solution. HEPES has poor buffering power at this pH, but similar results were observed with other buffers more appropriate for low pH. This finding suggests that the observed effects were induced by H^+ and were not a direct effect of the buffer itself. In Fig. 1, the decreased $I_{K,ATP}$ reached a stable value within 2 min after the solution was changed, but channel activity subsequently ceased completely at about 5 min after the solution change. In the same patch, a later return to a pH 7.4 solution restored the channel activity. In some patches the channel activity could not be restored after being reperfused with a pH 7.4 solution, but could be reactivated by a short exposure to 2 mM Mg-ATP. Pooled data from 42 patches, which were held at −60 or −80 mV and in either HEPES or acetic acid buffer, showed that 76 ± 4% of the channels in a patch became inactivated at 3 min in pH 4.5, compared with those active in pH 7.4. For the study of subconductance states, we selected patches containing only a single active channel that was not inactivated at low pH during a period from 30 sec to 5 min after the solution change to low pH. Effective solution change was judged by a characteristic decrease in unitary current amplitude. With this experimental protocol, we found that internal H^+ not only decreased $I_{K,ATP}$, but also induced subconductance states of $I_{K,ATP}$ (Fig. 1). Although subconductance states of $I_{K,ATP}$ have been previously reported at physiological pH_i (Kakei, Noma, & Shibasaki, 1985), we were unable to identify subconductance events in our records at pH_i 7.4 for membrane potentials from −100 to +60 mV, and with either $[K^+]_o/[K^+]_i$ = 144/144 (mM/mM) (23 experiments), or $[K^+]_o/[K^+]_i$ = 144/10 (mM/mM) (15 experiments). When pH_i was decreased to less than 6.5, however, we often recorded long sojourns at subconductance levels clearly distinct from the main current level. For those patches in which channels remained active, the subconductance levels disappeared upon return to a pH 7.4 solution (12 patches).

Multiple Levels of Subconductance

Careful examination of the experimental current records reveals that the low pH_i-induced subconductance events contained multiple subconductance levels. Figure 2*A* shows a length of current record at a membrane potential of −80 mV, pH_i 5.0, and $[K^+]_o/[K^+]_i$ = 144/10 (mM/mM), where two subconductance levels could be identified. To separate subconductance levels from overlap with background noise in the histograms, we used the mean-variance analysis method to measure the current values at the subconductance levels. Figure 2*B* plots mean-variance against current, and Fig. 2*C* shows the reorganized amplitude histogram after passing the data through the threshold determined from the mean-variance analysis. Two nearly equally spaced subconductance levels, S1 at 63% and S2 at 33% of the main current amplitude, are shown in Fig. 2*C*. Similar results were obtained from five other patches and they are summarized in the single channel current-voltage curves plotted in Fig. 3. The ratios of the amplitudes of the subconductance levels remain

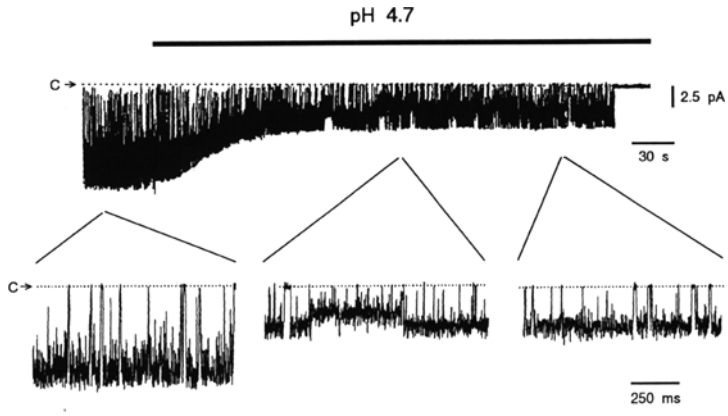

Fig. 1. The effect of internal acidification on single channel currents of an ATP-sensitive K^+ channel in an inside-out patch at membrane potential (V_m) of −80 mV. $[K^+]_o/[K^+]_i$ was 144 mM/144 mM. The internal solution contained HEPES 5 mM in both pH. Control internal solution had a pH of 7.4. The bar over the current record indicates the period of application of an internal solution with pH 4.7. The current was reproduced through a pen-recorder, with a f_c = 250 Hz. Open channel activity is shown as a downward deflection from the closed level (shown as C→). The lower traces are expansions in the time scale of the current record (f_c = 0.5 kHz). Note that the middle, lower traces illustrate a H^+-induced subconductance event.

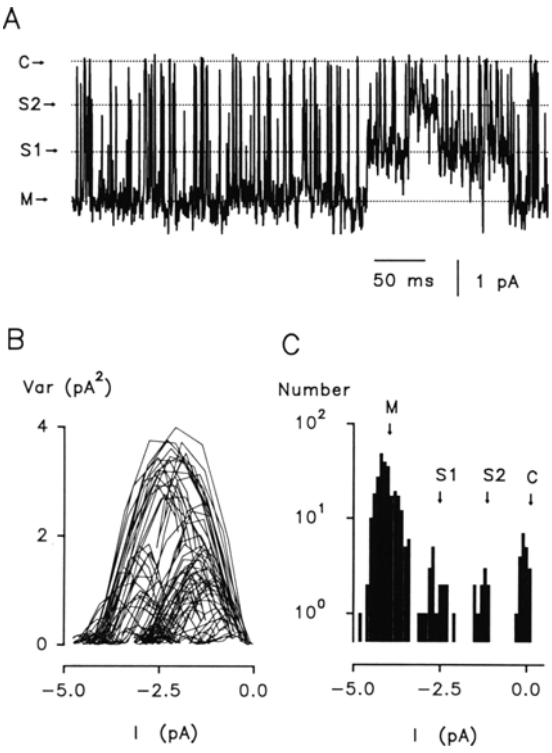

Fig. 2. Internal acidification induced $I_{K,ATP}$ subconductance levels. (*A*) Segment of current recording showing the main open level (M→), and two subconductance levels (S1→ and S2→). Open channel activity is shown as a downward deflection from the closed level (shown as C→). The recording was obtained at a V_m of −80 mV and pH_i 5.0, buffered with acetic acid 5 mM. $[K^+]_o/[K^+]_i$ was 144/10 (mM/mM), with sucrose 300 mM as substitution. (*B*) Mean-variance plot of the current recording containing subconductance levels. The ordinate is the variances of a six-point moving window, and the abscissa is the mean currents of the moving window. The plot shows four current levels, including the main open level, two subconductance levels and the closed level. (*C*) Correspondent amplitude histogram after removal of the sample points with a variance larger than the variance of the baseline. The two peaks in the middle of the plot indicate the approximate current values of the subconductance level S1 and level S2, respectively. The ordinate is the number of sample points in the record having the plotted amplitude. f_c = 2 kHz.

nearly constant over the entire voltage range tested. We used an Eyring rate theory to model permeation of K^+ through the channel by fitting the model to experimental data presented in Fig. 3. A three-energy barrier, two-energy well, single occupancy, Eyring rate theory model (*see* Hille, 1975, and Spruce, Standen & Stanfield, 1987), was used to give the unbroken lines drawn on the current-voltage relationships for the different subconductance levels in Fig. 3. The model gives the full voltage dependence of the conductance and subconductance levels at pH 5, with alterations in the free energy parameters of the barriers and wells (values given in the figure legend) accounting for the different conductances. The extrapolated zero-current intercept of the three levels at pH 5.0 all fall within a narrow voltage range, indicating that they are likely to have similar ion selectivity for K^+ over other ions such as Cl^-. Also, no apparent differences could be identified in the rectification characteristics of the current at the three levels. Furthermore, the ratios of the current amplitudes of each subconductance level were not significantly changed over the pH range we tested (pH 4.0–pH 6.5).

In addition to the two subconductance levels described in Fig. 2, we also noticed that for some subconductance events, other levels of subconductance occurred. In most cases, the current amplitude of such subconductance events fluctuated heavily making characterization difficult (Fig. 4). In the example shown, which was recorded at a membrane potential of −80 mV, pH_i 4.5, and $[K^+]_o/[K^+]_i$ = 144/10 (mM/mM), the channel currents assume distinct subconductance levels at S1 and S2 between 3,072 and 3,481 msec, but the current fluctuates at about half of the main current level during the latter part of the third trace (beginning with 3,481 msec) and the fourth trace (Fig. 4). It may be that this level is caused by a rapid transition between levels S1 and S2, but this

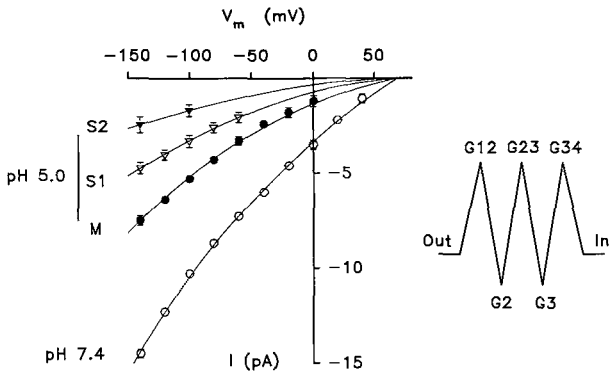

Fig. 3. Current-voltage relationship of two H^+-induced subconductance levels of single channel $I_{K,ATP}$. The single channel currents were recorded at different V_m in pH_i 7.4 (○), and in pH_i 5.0 ((M,●): main level, (S1,▽): subconductance level 1, (S2,▼): subconductance level 2). $[K^+]_o/[K^+]_i$ was 144/10 (mM/mM), with sucrose 300 mM substitution. The unbroken lines are fits to a three energy barrier, two energy well, single occupancy, Eyring rate theory model for K^+ permeation of the pore (*see* Hille, 1975). The rate constants for the transitions across the barriers are functions of the wells and barriers:

$$k_{12} = K_o{}^*Q^*e^{(-G12-V^*\delta)}$$
$$k_{21} = Q^*e^{(-G12+G2+V^*\delta)}$$
$$k_{23} = Q^*e^{(-G23+G2-V^*\delta)}$$
$$k_{32} = Q^*e^{(-G23+G3+V^*\delta)}$$
$$k_{31} = Q^*e^{(-G34+G3-V^*\delta)}$$
$$k_{13} = K_i{}^*Q^*e^{(-G34+G3-V^*\delta)}$$

where $V = V_m{}^*F/RT$, $K_i = 0.01$ M, $K_o = 0.14$ M, $Q = 6.21 \times 10^{23}S^{-1}$, $\delta = 0.167$ (dimensionless). The fractional occupancies of wells 2 and 3 are given by:

$$S2 = (k_{13}{}^*k_{32} + k_{12}{}^*k_{32} + k_{12}{}^*k_{31})/k$$
$$S3 = (k_{13}{}^*k_{21} + k_{13}{}^*k_{23} + k_{12}{}^*k_{23})/k,$$

where

$$k = k_{13}{}^*k_{21} + k_{13}{}^*k_{23} + k_{13}{}^*k_{32} + k_{12}{}^*k_{23} + k_{12}{}^*k_{32} + k_{12}{}^*k_{31} + k_{21}{}^*k_{32} + k_{31}{}^*k_{21} + k_{31}{}^*k_{23}$$

The current flow I (in pA) is then given by the net flow over barrier G23:

$$I = (S3{}^*k_{32} - S2{}^*k_{23}){}^*10^{-12}.$$

The model equations potentially had five free parameters: two energy wells G2 and G3, and three barriers G12, G23, and G34 (depicted diagrammatically in the inset on the right) and the electrical distance δ for G2 was fixed at 0.167 in agreement with the Spruce et al. (1987) model for $I_{K,ATP}$. The model equations were fit using the least-squares nonlinear regression routine NLIN in the SAS (Cary, NC) statistical software running on a SUN ELC workstation. For pH 7.4 (○), the values for G2, G3, G12, G23 and G34 were −2.3, −7.6, 6.1, 5.8 and 4.3, respectively. At pH 5, the values for G2, G12, G23 and G34 were fixed at −1.8, 5.0, 10.5, 7.0, respectively, and G3 alone was allowed as a free parameter of the fit. The well depth for G3 was −4.0, −5.4, and −6.5 for the M, S1, and S2 conductance levels, respectively. Each data point is the mean from 3–10 measurements. SEM for each mean is presented as a bar where it is larger than the symbol.

explanation seems less likely for the two events at about 3,850 msec.

Subconductance as a Function of pH, Membrane Potential and Ionic Strength

The relative probability of the subconductance states is increased with a decrease of pH_i. We defined the relative probability as the sojourn time at subconductance levels (nonmain level) as a fraction of the total channel open times within a record. Figure 5*A* shows the pH_i dependence of the probability of occurrence of subconductance levels from 13 patches. The membrane potential was between −60 and −100 mV with $[K^+]_o/[K^+]_i = 144/10$ (mM/mM). The variability of the data in both panels of Fig. 5 may be explained by the difficulty in maintaining channel activity in low pH_i which caused data to be collected from different durations of recording. A general fit of a one-order Hill function to the data gives a $pH_i = 4.9$ at half-maximal effect with the maximal probability of the occurrence of subconductance states at 0.26. In the analysis of the relative probability of the occurrence of subconductance levels, we did not measure the relative occurrence of the individual subconductance levels because of the uncertainty in recognizing them under some circumstances (such as in the case of Fig. 4). By inspection, however, the 33% subconductance level (S2) seemed to occur much less often than the 63% subconductance level (S1).

Summary data for the dependence of the occurrence of subconductance levels on ionic strength at two potentials are summarized in Fig. 5*B*. Sucrose was used to substitute for K^+ to yield $[K^+]_i$ of 10 mM. The occurrence of subconductance levels induced by internal H^+ was greater for the lower ion strength solutions, and has a slight voltage-dependence.

For membrane potentials positive to the reversal potential, the small amplitude of outward unitary current caused by inward rectification at low pH made it difficult to resolve subconductance events. It appeared that outward current showed fewer subconductance events compared with inward current, but the difficulty in resolving these events prevented detailed analysis.

Relationship between Subconductance and Other Possible Conformation Changes of the Channel

To gain insight into potential mechanisms for the induction of subconductance levels, we studied (i) the kinetic characteristics of the channel during the

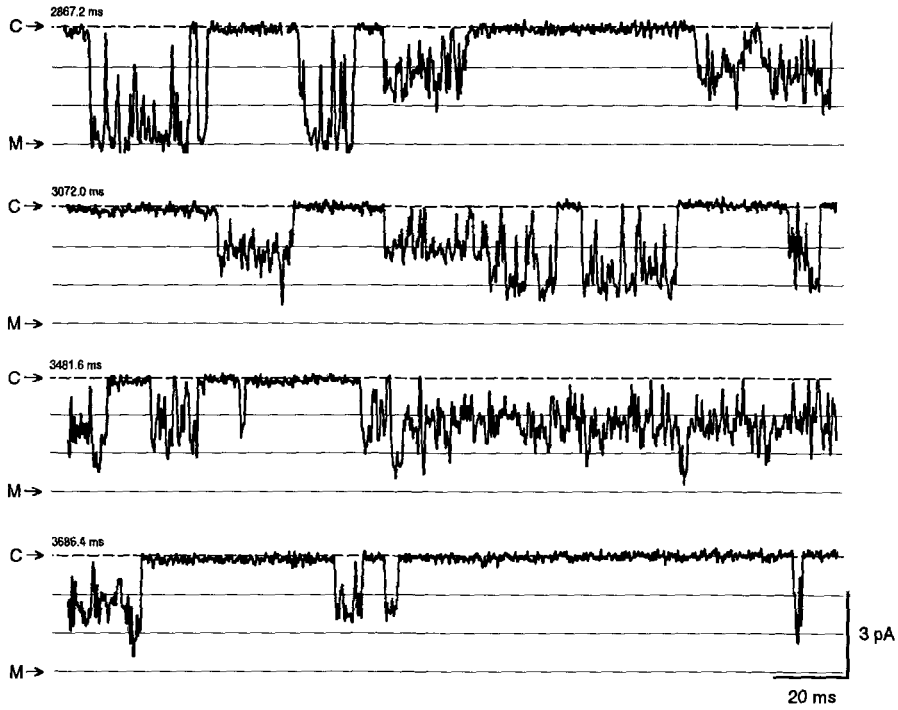

Fig. 4. Internal acidification induced multiple subconductance states of $I_{K,ATP}$: fluctuation between subconductance levels. The recording was obtained at a V_m of −80 mV and pH_i 4.5 buffered with acetic acid 5 mM. $[K^+]_o/[K^+]_i$ was 144/10 (mM/mM), with sucrose 300 mM substitution. f_c = 2 kHz. The four traces were from a continuous record. The continuous lines between the main level and the closed level are drawn at 33 and 67% of the main level, respectively. The numbers at the beginning of each trace are the time after the recording started.

subconductance states in comparison with that during the main level, and (ii) the influence of rundown and trypsin modification on the occurrence of the subconductance induced by H^+.

The gating of the cardiac $I_{K,ATP}$ channel has been shown to be composed of only a single transition between an open state and a closed state in the absence of both ATP and rundown (Qin, Takano & Noma, 1989; Fan, Nakayama & Hiraoka, 1990*b*). We analyzed this transition during the subconductance levels in comparison with that during the main levels. In some of our experimental recordings the sojourn time in the subconductance level S1 was so long (Fig. 6A) that enough open/closed events could be collected to form open time and closed time histograms of the subconductance level S1 compared with the main level (Fig. 6*B*). For these results recorded at a membrane potential of −80 mV with $[K^+]_o/[K^+]_i$ = 144/10 (mM/mM), the histograms for the main level and the subconductance level were nearly superimposed. The same result was a consistent finding in all cases where the analysis could be made and no statistically significant difference could be found. For data from six experiments, at three membrane potentials (−80, −140, and −50 mV, the paired *t*-test for the overall differences was not significant for both open and closed time constants. Therefore, the occurrence of subconductance states appears not to induce an alternation in channel open kinetics in the absence of ATP, at least under the conditions of these experiments. For subconductance level S2, the kinetics analysis was apparently more difficult to apply because of the smaller current amplitude and larger open channel noise.

We noticed that subconductance levels also appeared at low pH_i during rundown. The record in Fig. 4 was taken from a patch that had channel open probability reduced by rundown. Subconductance levels are clearly demonstrated. Whatever process causes rundown, it appears not to affect the mechanism for the induction of subconductance levels.

Digestion of the cytoplasmic side of the membrane with trypsin can remove the cation-induced inhibition of the channel (Fan & Makielski, 1993; Furukawa et al., 1993), sulfonylurea block of the channel (Nichols & Lopatin, 1993), and reveals the antagonism of low pH_i on ATP inhibition (Fan & Makielski, 1993). These trypsin digestion effects may be caused by cleavage of a hydrophilic part or parts of the channel protein on the cytoplasmic side of the membrane. In A-type K^+ channels, trypsin digestion removes a peptide of 20 amino acids from the cytoplasmic side of the channel (Hoshi, Zagotta & Aldrich, 1990). This peptide is the putative "ball and chain" which functions as a blocker of the channel entrance. Trypsin cleavage does not prevent the occurrence of the subconductance levels induced by low pH_i (Fig. 7). The patch was treated with trypsin (2 mg/ml) for 15 min, and after washout of trypsin, a channel was continuously opening in the absence of ATP at pH 7.4 (Fig. 7). No subconductance levels were observed during the period at pH 7.4. Addition

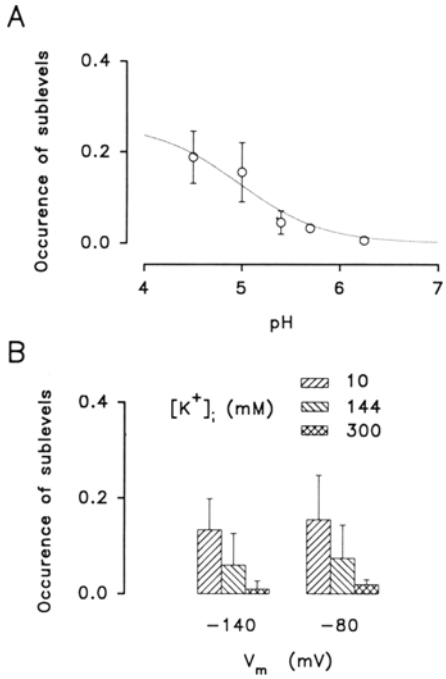

Fig. 5. (*A*) pH dependence of the probability of the occurrence of $I_{K,ATP}$ subconductance levels. The probability of occurrence was expressed as the fraction of the sum of the sojourn time at all recognizable subconductance levels over the sum of the total open time for a record of 30–90 sec. Single channel $I_{K,ATP}$ was recorded at V_m between −60 and −80 mV. $[K^+]_o/[K^+]_i$ was 144/10 (mM/mM), with sucrose 300 mM substitution. The line is a fit to a Hill function

$$0.28([H]_i/([H]_i + 10^{-4.9})$$

(*B*) The influences of ionic strength and membrane potential on the occurrence of $I_{K,ATP}$ subconductance levels induced by H^+. The occurrence of subconductance states in $[K^+]_i$ 300, 144 and 10 mM were measured at membrane potentials of −80 and −140 mV. The data were presented as mean ± SEM with 3–5 measurements for each data.

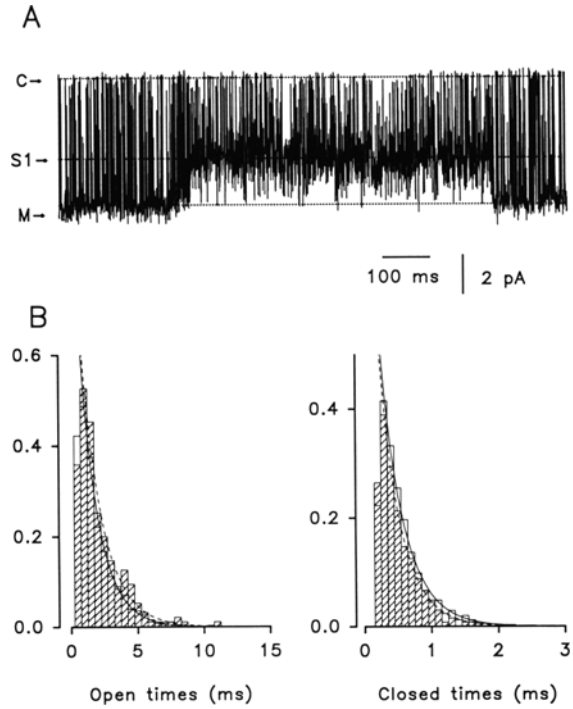

Fig. 6. Comparison of the gating kinetics of $I_{K,ATP}$ during a subconductance state with the kinetics during the main conductance state. (*A*) Current recorded from an inside-out membrane patch with pH_i 5.9 buffered with MES 5 mM. The recording was obtained at a V_m of −80 mV, and $[K^+]_o/[K^+]_i$ was 144/10 (mM/mM), with sucrose 300 mM as substitution. f_c = 2 kHz. (*B*) Histograms of open (left) and closed (right) times for the main conductance and the subconductance level are superimposed. The lines are best fits to single exponential distributions, and are: 1.43 and 0.35 msec for the main state (continuous line); 1.6 and 0.33 msec for the subconductance state (broken lines). The ordinate for the histograms is normalized to 1 at time 0.

of 0.5 mM ATP to the internal solution closed the channel. Lowering pH_i to 5.7 in the presence of ATP (0.5 mM) opened the channel, consistent with our previous report (Fan & Makielski, 1993). At the same time, the unitary current started to alternate between subconductance levels and the main level (*see* recording of subconductance level S1 between 7,196–7,700 msec in Fig. 7). The subconductance events were not observed after return to ATP-free and pH 7.4 solution (*record not shown*).

Finally, we tested the effect of external acidification on $I_{K,ATP}$. $I_{K,ATP}$ was completely insensitive to the external acidification. We observed no subconductance events, nor significant changes in unitary conductance, nor changes in gating kinetics of $I_{K,ATP}$ at pH_o 3.0–4.0 in comparison with pH_o 7.4 in the absence of ATP in the internal solution (four experiments).

Discussion

The major findings of this study are that (i) cytoplasmic acidosis induces subconductance of cardiac $I_{K,ATP}$ channels, (ii) the subconductance levels are multiple with two major subconductance levels equally spaced between the main open level and closed level, and (iii) the occurrence of the subconductance states appears to be independent of channel gating, channel available states inactivated by rundown of the channel and trypsin digestion, but dependent upon pH, cytoplasmic ion strength, and also slightly on membrane potential.

Subconductance States of $I_{K,ATP}$ Channels

Subconductance is a common phenomena among various types of ion channels (*see* Fox, 1987, for

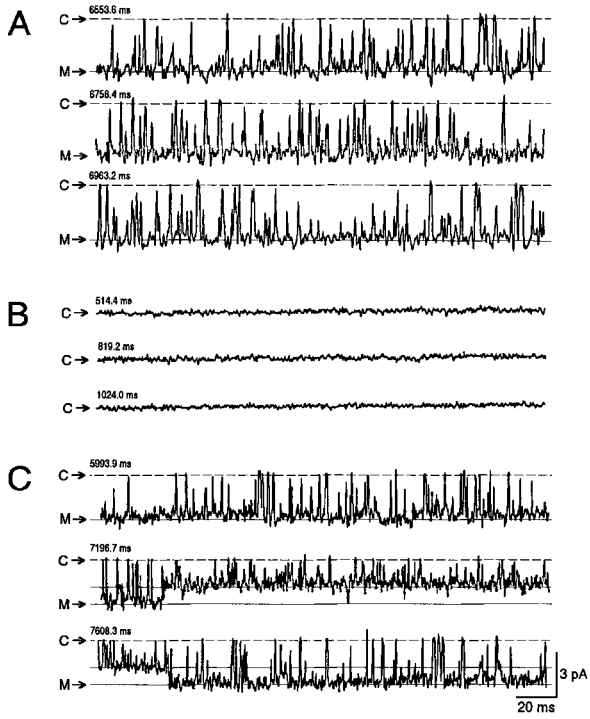

Fig. 7. H^+ – induced subconductance states of $I_{K,ATP}$ in trypsin-treated patches. (*A*), (*B*) and (*C*) were recorded from the same inside-out patch. The cytoplasmic side of the patch was pretreated by 2 mg/ml trypsin for 15 min. (*A*) is in the ATP-free, pH 7.4 internal solution, (*B*) is in the presence of 0.5 mM ATP at pH 7.4, and (*C*) is in the presence of 0.5 mM ATP at pH 5.7 buffered with PIPES 5 mM. $[K^+]_o/[K^+]_i$ was 144/144 (mM/mM). Membrane potential was −50 mM and f_c = 2 kHz. Open channel activity is shown as a downward deflection from the closed level (shown as C→) and the main open level (M→). In (*C*), the continuous line between the main level and the closed level is drawn at 63% of the main level which represents the value of one of the subconductance states form the mean-valance histogram. The numbers at the beginning of each trace are the time after the recording started.

review). Although $I_{K,ATP}$ channels have been widely studied in many tissues, including cardiac myocytes, pancreatic β-cells, skeletal myocytes, central neurons, smooth muscle cells, renal epithelial cells, and even on mitochondrial inner membranes (*see* Ashcroft & Ashcroft, 1990, for review), subconductance states of these channels have not been well defined. Few studies report subconductance levels of these channels. In the study of Kakei et al. (1985) on cardiac cells, various levels of subconductance states were reported at normal pH_i, but their relative rarity precluded detailed analysis. Similar subconductance events were also observed in a recent report on $I_{K,ATP}$ from human ventricular myocytes at pH_i 7.2 (Babenko et al., 1992), but again no detailed analysis was done. In the $I_{K,ATP}$ channel of rat skeletal muscle fibers, multiple subconductance levels appeared after adding and withdrawing the channel blocker adenine to the cytoplasmic side of the membrane (Weik, Lönnendonker & Neumcke, 1989). Because adenine blocks the channel itself, possibly by binding to the nucleotide block site, the subconductance levels could only be observed transiently upon removal of adenine. A common characteristic between the subconductance induced by H^+ we observed and the earlier reports is the existence of multiple subconductance levels for $I_{K,ATP}$ channels. Kakei et al. (1985) described subconductance levels that varied between 20 to 90% of the main level, and Weik et al. (1989) found subconductance levels at 1/4, 1/2, 3/4, 1/6, 1/3 and 2/3 of the main level. We found two major subconductance levels of 33 and 63% of the main conductance. Subconductance events at other current levels, especially at about half of the main level, also appeared, but we were not able to determine their actual levels because of their large fluctuations (*see* Fig. 4).

Conformation Changes as a Mechanism for pH_i-Induced Subconductance States

It has been suggested that there are two major types of subconductance behavior (Fox, 1987; Dani & Fox, 1991). The first type of subconductance behavior is characterized by conductance levels that have no obvious numerical relationship to the main conductance level, while the second type is characterized by conductance levels that are equally spaced at some fraction of the main conductance. Equally spaced subconductance levels strongly suggest that the channel is an oligo-channel complex composed of several identical pores. The *Torpedo* Cl^- channel behaves as a dimeric pore composed of identical proto-channels (Miller, 1982), and the K^+ inward rectifier channel in heart behaves as a trimeric pore as revealed by blocking ions (Matsuda, 1988). Unequally spaced subconductance levels are usually explained by the mechanism of partial opening and closing of the ion conducting pathway.

Ionic block of equally spaced subconductance levels can yield evidence supporting the hypothesis of a multi-barrel channel model (Miller & White, 1984; Matsuda & Noma, 1989). Our data show that H^+ induced the appearance of two major subconductance levels which are nearly equally spaced between the main level and the closed level, suggesting a multiple-barrel model. On the other hand, we also find evidence against such a model. We observed subconductance levels other than those that were $\frac{1}{3}$ and $\frac{2}{3}$ of main level. Moreover, none of the well-studied open channel blockers of $I_{K,ATP}$ such as Mg^{2+}, Na^+, Cs^{2+}, Ba^{2+}, and pinacidil (Horie, Irisawa

& Noma, 1987; Quayle, Standen & Stanfied, 1988; Fan et al., 1990*a*), acting either from the inside or outside of the membrane, has been reported to induce the appearance of subconductance states of $I_{K,ATP}$ channels. Despite intensive study, other channel blockers such as nucleotides, sulfonylurea, TEA, 4-AP, quinine and quinidine, also have never been reported to induce subconductance states (for reviews about blocking effects, *see* Ashcroft, 1988; Ashcroft & Ashcroft, 1990; Davies, Standen & Stanfield, 1991; Nichols & Lederer, 1991; for examples of particular studies, *see* Kakei, et al., 1985; Davies, Standen & Stanfield, 1989; Gillis et al., 1989; Undrovinas et al., 1990). Adenine-induced subconductance states are an exception.

H^+-induced subconductance levels in the Ca^{2+} channel have been explained by a completely different mechanism. Quantitative analysis of H^+-induced Ca^{2+} channel current subconductance level suggested H^+ binding to a site outside the pore that induced a conformational change affecting permeation (Pietrobon, Prod'hom & Hess, 1989; Prod'hom, Pietrobon & Hess, 1989). The same mechanism was also applied to model Zn^{2+}-induced subconductance states in the Na^+ channel (Schild, Ravindran & Moczydlowski, 1991). We could not, however, apply the model analysis to our observation of H^+-induced subconductance of $I_{K,ATP}$ because of the multiple subconductance levels and the difficulty in determining the subconductance levels. We nevertheless speculate that formation of the multiple subconductance levels we observed for the cardiac $I_{K,ATP}$ channel, even though they (or some of them) consist of equally spaced subconductance levels, are probably induced by a partial opening/closure of a single channel pore. The partial opening/closure may be caused by a slight deformation of the ion pore caused by a channel conformation change, rather than by being blocked by a hydrophilic peptide, such as a "ball and chain" model (Bezanilla & Armstrong, 1977). The insensitivity of the subconductance states to trypsin digestion supports this view although it does not prove it. Recent pore model simulations indicate that slight alterations of the energy profile in a single pore can also produce equally spaced subconductance levels, which have the same selectivity and binding affinities as the main conductance level (Dani & Fox, 1991). We used an Eyring rate theory to model permeation of K^+ through the channel by fitting the model to experimental data presented in Fig. 3. The model, which uses three energy barriers and two energy wells with a single ion occupation at a time (Spruce et al., 1987), was used to give the unbroken lines drawn on the current voltage relationships for the different subconductance levels in Fig. 3. The model gives the full voltage dependence of the conductance and subconductance levels at pH 5 with alterations in the free energy parameters of the barriers and wells (values given in the figure legend) accounting for the different conductances. To constrain the model, we fixed all but the inner well (G3) to have common values for the three conductance levels at low pH. With this fit, the decreased conductance for the subconductance states was easily explained by a fit having a progressively deeper well. This model is not definitive, and indeed even within this one model the choice to vary G3 was arbitrary, but it does show that conformational changes affecting a single well can easily account for the observed subconductance levels. The data also cannot distinguish whether the possible conformation change is induced by specific H^+ binding to a binding site or whether the peptide structure changes in response to the surrounding solvent pH. The dependence of the occurrence of a subconductance state on the ionic strength and membrane potential, however, suggests a role of negative surface charge at the vicinity of inner entrance of ionic pore in the H^+-induced subconductance state.

Possible Kinetic Models for the Subconductance States

Although our present data do not allow us to propose a quantitative kinetic model for gating, we have attempted to explain the subconductance states with a minimized three-state model based on our qualitative observations. We first assume that there are only two major subconductance levels, S1 and S2, and for simplicity, we have eliminated consideration of the closed state. The three-state model has potentially two different sequential arrangements (Fig. 8*A* and *B*). These arrangements cannot account for the transitions between subconductance levels that we observed because they either do not allow for direct transitions between S2 and the main conductance level (M) as in arrangement *A*, or they do not allow transition between S1 and S2 (arrangement *B*). We found direct transitions between all three levels in our data. Arrangement *C* appears suitable because it allows for direct transitions between all three states. This closed model has been used to describe the transitions of multiple conductance states (Hill, Coronado & Strauss, 1990), yet it may not be satisfactory for our results. In this model, at least one of the transition rates leaving state M should be a linear function of proton concentration to explain the pH-dependent occurrence of the subconductance states. Such a pH-dependent transition would eventually lead to sojourning in the subconductance states

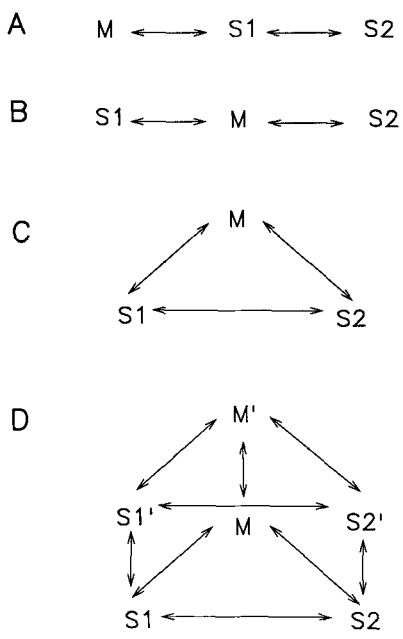

Fig. 8. Putative kinetic models to explain subconductance states of $I_{K,ATP}$. *See text for details.*

100% of the time. In our experiments, we never found the proportion of subconductance openings to be greater than 50% of the fraction of subconductance levels over total opening times. Our range of test pH_i might be considered limited and perhaps the Hill model is not the correct one to extrapolate, but the data in Fig. 5*A* suggest that, even at very low pH, the system will not move toward a predominance of subconductance states. A more complicated model such as the one in arrangement *D* (Fig. 8), in which protons facilitate and modulate transitions between three states, may be required to account for the data.

Physiological Relevance

Although cytoplasmic acidosis increases $I_{K,ATP}$ through antagonizing ATP inhibition of the channel in the presence of ATP, it decreases $I_{K,ATP}$ through reducing unitary current and open probability in the absence of ATP. The H^+-induced subconductance states we report here represent a novel, third mechanism by which acidosis might reduce $I_{K,ATP}$. However, because the H^+-induced subconductance events reach half-maximal occurrence at pH_i as low as 4.9, and because at maximum the occurrence of these states was only about 30%, it is hard to predict what the physiological function of such subconductance states might be. In one experiment, we have occasionally seen that in the presence of ATP, the subconductance state S2 had longer open bursting durations than those of the main level at pH_i 6.5. It will be interesting to see whether the subconductance levels have an ATP sensitivity that differs from that of the main level. Subconductance states of a channel can have significantly different functional behavior than the main open state, such as differences in sensitivity to blockers (Takeda & Trautmann, 1984; Sunami et al., 1993). Further experiments on subconductance levels of $I_{K,ATP}$ will be necessary to address these questions for this channel.

This work was supported by a grant from the Ministry of Education, Science and Culture of Japan to M.H. and a grant from the National Institutes of Health (PO1 HL20592) to J.C.M. Dr. Makielski is an Established Investigator of the American Heart Association.

References

Ashcroft, F.M. 1988. Adenosine 5'-triphosphate-sensitive potassium channels. *Annu. Rev. Neurosci.* **11**:97–118

Ashcroft, S.J.H., Ashcroft, F.M. 1990. Properties and functions of ATP-sensitive K-channels. *Cell. Signall.* **2**:197–214

Babenko, A.P., Samoilov, V.O., Kazantseva, S.T., Shevchenko, Y.L. 1992. ATP-sensitive K^+-channels in the human adult ventricular cardiomyocytes membrane. *FEBS Lett.* **313**:148–150

Bezanilla, F., Armstrong, C.M. 1977. Inactivation of the sodium channel I. Sodium current experiments. *J. Gen. Physiol.* **70**:549–566

Christensen, O., Zeuthen, T. 1987. Maxi K^+ channels in leaky epithelia are regulated by intracellular Ca^{2+}, pH and membrane potential. *Pfluegers Arch.* **408**:249–259

Cook, D.L., Ikeuchi, M., Fujimoto, W.Y. 1984. Lowering of pH_i inhibits Ca^{2+}-activated K^+ channels in pancreatic β-cells. *Nature* **311**:269–271.

Cuevas, J., Bassett, A.L., Cameron, J.S., Furukawa, T., Myerburg, R.J., Kimura, S. 1991. Effect of H^+ on ATP-regulated K^+ channels in feline ventricular myocytes. *Am. J. Physiol.* **261**:H755–H761

Dani, J.A., Fox, J.A. 1991. Examination of subconductance levels arising from a single ion channel. *J. Theor. Biol.* **153**:401–423

Davies, N.W. 1990. Modulation of ATP-sensitive K^+ channels in skeletal muscle by intracellular protons. *Nature* **343**:375–377

Davies, N.W., Standen, N.B., Stanfield, P.R. 1991. ATP-dependent potassium channels of muscle cells: their properties, regulation, and possible functions. *J. Bioenerg. Biomembrane* **23**:509–535

Davies, N.W., Standen, N.B., Stanfield, P.R. 1989. Multiple blocking mechanisms of ATP-sensitive potassium channels of frog skeletal muscle by tetraethylammonium ions. *J. Physiol.* **413**: 31–47

Davies, N.W., Standen, N.B., Stanfield, P.R. 1992. The effect of intracellular pH on ATP-dependent potassium channels of frog skeletal muscle. *J. Physiol.* **445**:549–568

El-Sherif, N., Fozzard, H.A., Hanck, D.A. 1992. Dose-dependent modulation of the cardiac sodium channel by the sea anemone toxin ATXII. *Circ. Res.* **70**:285–301

Fabiato, A., Fabiato, F. 1979. Calculator programs for computing the composition of the solutions containing multiple metals and ligand used for experiments in skinned muscle cells. *J. Physiol. (Paris)* **75**:463–505

Fan, Z., Makielski, J.C. 1993. Intracellular H^+ and Ca^{2+} modulation of trypsin-modified ATP-sensitive K^+ channels in rabbit ventricular myocytes. *Circ. Res.* **72**:715–722

Fan, Z., Nakayama, K., Hiraoka, M. 1990*a*. Multiple actions of pinacidil on adenosine triphosphate-sensitive potassium channels in guinea-pig ventricular myocytes. *J. Physiol.* **430**:273–295

Fan, Z., Nakayama, K., Hiraoka, M. 1990*b*. Pinacidil activates the ATP-sensitive K^+ channel in inside-out and cell-attached patch membranes of guinea-pig ventricular myocytes. *Pfluegers Arch.* **415**:387–394

Fox, J.A. 1987. Ion channel subconductance states. *J. Membrane Biol.* **97**:1–8

Furukawa, T., Fan, Z., Sawanobori, T., Hiraoka, M. 1993. Modification of the adenosine 5′-triphosphate-sensitive K^+ channel by trypsin in guinea-pig ventricular myocytes. *J. Physiol.* **466**:707–726

Gillis, K.D., Gee, W.M., Hammoud, A., McDaniel, M.L., Falke, L.C., Misler, S. 1989. Effects of sulfonamides on a metabolite-regulated ATP-sensitive K^+ channel in rat pancreatic β-cells. *Am. J. Physiol.* **257**:C1119–C1127

Hill, J.A., Coronado, R., Strauss, H.C. 1990. Open-channel subconductance state of K^+ channel from cardiac sarcoplasmic reticulum. *Am. J. Physiol.* **258**:H159–H164

Hille, B. 1975. Ionic selectivity, saturation, and block in sodium channels: a four barrier model. *J. Gen. Physiol.* **66**:535–560

Horie, M., Irisawa, H., Noma, A. 1987. Voltage-dependent magnesium block of adenosine-triphosphate-sensitive potassium channel in guinea-pig ventricular cells. *J. Physiol.* **387**:251–272

Hoshi, T., Zagotta, W.N., Aldrich, R.W. 1990. Biophysical and molecular mechanisms of Shaker potassium channel inactivation. *Science* **250**:533–538

Ito, H., Vereecke, J., Carmeliet, E. 1992. Intracellular protons inhibit inward rectifier K^+ channel of guinea-pig ventricular cell membrane. *Pfluegers Arch.* **422**:280–286

Kakei, M., Noma, A., Shibasaki, T. 1985. Properties of adenosine-triphosphate-regulated potassium channels in guinea-pig ventricular cells. *J. Physiol.* **363**:441–462

Matsuda, H. 1988. Open-state substructure of inwardly rectifying potassium channels revealed by magnesium block in guinea-pig heart cells. *J. Physiol.* **397**:237–258

Matsuda, H., Noma, A. 1989. Triple-barrel structure of inwardly rectifying K^+ channels revealed by Cs^+ and Rb^+ block in guinea-pig heart cells. *J. Physiol.* **413**:139–157

Miller, C. 1982. Open-state substructure of single chloride channels from *Torpedo* electroplax. *Phil. Trans. R. Soc. Lond. B* **299**:401–411

Miller, C., White, M. 1984. Dimeric structure of single chloride channels from *Torpedo* electroplax. *Proc. Natl. Acad. Sci. USA* **81**:2772–2775

Misler, S., Gillis, K., Tabcharani, J. 1989. Modulation of gating of a metabolically regulated, ATP-dependent K^+ channel by intracellular pH in β cells of the pancreatic islet. *J. Membrane Biol.* **109**:135–143

Moody, W. 1984. Effects of intracellular H^+ on the electrical properties of excitable cells. *Annu. Rev. Neurosci.* **7**:257–278

Nichols, C.G., Lederer, W.G. 1991. Adenosine triphosphate-sensitive potassium channels in the cardiovascular system. *Am. J. Physiol.* **261**:H1675–H1686

Nichols, C.G., Lopatin, A.N. 1993. Trypsin and α-chymotrypsin treatment abolishes glibenclamide sensitivity of K_{ATP} channels in rat ventricular myocytes. *Pfluegers Arch.* **422**:617–619

Patlak, J.B. 1988. Sodium channel subconductance levels measured with a new variance-mean analysis. *J. Gen. Physiol.* **92**: 413–430

Pietrobon, D., Prod'hom, B., Hess, P. 1989. Interactions of protons with single open L-type calcium channels. *J. Gen. Physiol.* **94**:1–21

Prod'hom, B., Pietrobon, D., Hess, P. 1989. Interactions of protons with single open L-type calcium channels. Location of protonation site and dependence of proton-induced current fluctuations on concentration and species of permeant ion. *J. Gen. Physiol.* **94**:23–42

Qin, D., Takano, M., Noma, A. 1989. Kinetics of ATP-sensitive K^+ channel revealed with oil gate concentration jump method. *Am. J. Physiol.* **257**:H1624–H1633

Quayle, J.M., Standen, N.B., Stanfield, P.R. 1988. The voltage-dependent block of ATP-sensitive potassium channels of frog skeletal muscle by caesium and barium ions. *J. Physiol.* **405**:677–697

Schild, L., Ravindran, A., Moczydlowski, E. 1991. Zn^{2+}-induced subconductance events in cardiac Na^+ channels prolonged by batrachotoxin—current voltage behavior and single-channel kinetics. *J. Gen. Physiol.* **97**:117–142

Spruce, A.E., Standen, N.B., Stanfield, P.R. 1987. Studies of the unitary properties of adenosine-5′-triphosphate-regulated potassium channels of frog skeletal muscle. *J. Physiol.* **382**:213–236

Standen, N.B., Pettit, A.I., Davies, N.M., Stanfield, P.R. 1992. Activation of ATP-dependent K^+ currents in intact skeletal muscle fibres by reduced intracellular pH. *Proc. R. Soc. Lond. [Biol].* **247**:195–198

Sunami, A., Sasano, T., Matsunaga, A., Fan, Z., Sawanobori, T., Hiraoka, M. 1993. Properties of veratridine-modified single Na^+ channels in guinea pig ventricular myocytes. *Am. J. Physiol.* **264**:H454–H463

Takeda, K., Trautmann, A. 1984. A patch-clamp study of the partial agonist actions of tubocurarine on rat myotubes. *J. Physiol.* **349**:353–374

Undrovinas, A.I., Burnashev, N., Eroshenko, D., Fleidervish, I., Starmer, C.F., Makielski, J.C., Rosenshtraukh, L.V. 1990. Quinidine blocks adenosine 5′-triphosphate-sensitive potassium channels in heart. *Am. J. Physiol.* **259**:H1609–H1612

Weik, R., Lönnendonker, U., Neumcke. 1989. Low-conductance states of K^+ channels in adult mouse skeletal muscle. *Biochim. Biophys. Acta* **983**:127–134